# Bulk-Edge Correspondence in the 1D SSH Model

Dhruv Kush,
Department of Physics & Astronomy, University of British Columbia, B.C, V6T 1S1, Canada

(Dated: December 13th, 2021)

The much celebrated bulk-edge correspondence states that whenever a system has certain non-zero topological invariants, it allows for edge states, robust to adiabatic transformations of the Hamiltonian, to exist. A general proof of this correspondence does not exist and even proofs for specific systems are difficult. In this article, we present the ingredients of a simple proof of said correspondence for the 1D Su-Schrieffer-Heeger model - we show that the number of zero-energy edge modes, robust to adiabatic deformations, is equal to a topological invariant called the winding number. Moreover, we discuss additional considerations to construct a more general proof.

## I. WHAT IS THE BULK-EDGE CORRESPONDENCE?

Say, you have a model Hamiltonian for a system. Let us also say we apply periodic boundary conditions (PBC) to our Hamiltonian because the system is big enough for us to ignore boundary-effects or perhaps we are only interested in what is happening in the bulk. We begin by defining what edge states are. They are eigenstates of the Hamiltonian that are localized at the boundaries. It turns out that we can then compute certain integrals for the Hamiltonian that tell us how many robust (a term defined later) zero-energy edge states the system can exhibit. These integrals involve knowing about the spectrum of the Hamiltonian, which is typically done by imposing PBCs. It is a very surprising fact that calculations done on the bulk of the system, which means ignoring the boundaries by applying PBCs, can give us information about the edges. [1]

### A. Why is the bulk-edge correspondence useful outside of piquing the physicist's curiosity?

Two systems or Hamiltonians are considered topologically equivalent if they can be continuously and adiabatically transformed into one another. In mathematical language, two Hamiltonians are equivalent if and only if they are homotopic to each other [2]. When this is the case, we can characterize equivalent systems by certain integrals/quantities called topological invariants, appropriately named since their value remains the same for topologically equivalent systems. Thus, finding out which numbers help describe properties of the system and remain invariant under adiabatic transformations serves as a classification for equivalent systems.[3]

### B. What are the physical consequences of this mathematical notion of equivalence?

As an example of its power, we will show that the number of zero energy edge states in the generalized Su-Schrieffer-Heeger (SSH) model remains the same as we deform this Hamiltonian adiabatically. These zero-energy edge states can be shown to be the eigenstates of the newly deformed Hamiltonian as well. In literature, these states are said to be robust to adiabatic, continuous deformations of the Hamiltonian. For the SSH Model, we can show that non-zero energy edge states are not robust. So, robust edge states are non-zero energy edge states are interchangeable terms for our discussion. The number of robust edge states is equal to a quantity called the winding number, which remains invariant under these adiabatic transformations. Therefore, if we know that a different Hamiltonian is topologically equivalent to the SSH Hamiltonian, we immediately know how many zero energy edge states it has, since the winding number is a topological invariant characterizing the SSH and equivalent Hamiltonians.

The true power of this formalism lies in describing topological phase transitions, which are phase transitions that cannot be described by Laundau's theory of phase transitions. Landau's theory is a phenomenological one, in which one can explain a phase transition by minimizing a free energy functional that must obey the symmetries of the Hamiltonian. Not all phase transitions can be explained by using this formalism. Finding topological invariants and classifying Hamiltonians as equivalent helps us ascertain when certain phase transitions are possible and what symmetries (chiral, time-reversal, particle-hole symmetries) we end up preserving after such transitions. We will see one such example for the standard SSH Model in section III. For further examples on the different types of invariants (such as Chern numbers, Pffafians) and the power of topological classification of systems, we refer the interested reader to reference [4].

## II. PRELIMINARIES OF THE GENERALIZED SSH MODEL

### A. The Standard SSH Model in 1D

The SSH Model describes spinless fermions hopping on a lattice, where the unit cell has two inequivalent sites, $A$ and $B$. Here, we only consider the tight-binding part of the full SSH Model. If we allow for electron-phonon cou-

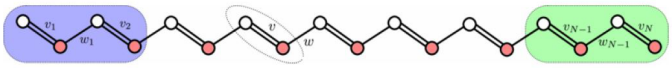

FIG. 1. Two Site Unit Cell in the Standard SSH Model. [6]

pling, the model describes the trans-polyacetylene structure. We must note that in the tight binding part of H, the charge transfer energy vanishes as both sites are thought to contain the same atom and have the same environment. [5] Fermions can hop from $A$ to $B$ and vice versa, but not from $A$ to $A$ or $B$ to $B$. The model we consider generalizes the hoppings from $A$ to $B$ to extend across unit cells, while disallowing $A$ to $A$ and $B$ to $B$ hoppings still. Thus, the system is called bipartite, and as we will see later, has chiral symmetry.

Let us first see how to diagonalize the standard SSH Model to obtain its momentum space representation and energy spectrum.

$$H = \sum_{n=1}^{N} (v_n c_{n,1}^\dagger c_{n,2} + w_n c_{n,2}^\dagger c_{n+1,1} + h.c)$$

Now, define:

$$c_n^\dagger = (c_{n,1}^\dagger, c_{n,2}^\dagger)$$

Keep in mind, $c_n$ is now a column vector with two entries. We can rewrite the Hamiltonian to get:

$$H = \sum_{n,m=1}^{N} c_m^\dagger H_{mn}^\circ c_n$$

We can show that $H_{mn}^\circ = 0$ for $|m-n| > 1$.
We assume discrete translation invariance in this system. From Bloch's theorem, we get that $c_n = e^{ik(n-1)a} c_1$

Then, $H = \begin{pmatrix} c_1^\dagger & .. & c_1^\dagger \end{pmatrix} (U + Te^{ika} + T^\dagger e^{-ika}) \begin{pmatrix} c_1 \\ c_1 \\ .. \end{pmatrix}$

Matrices $U$ and $T$ are defined below.

Now, in order for the Hamiltonian to be translation invariant, one may show that we need $w_n = w$ and $v_n = v$.

So, via discrete translation invariance, we have:

$$U_n = U = \begin{pmatrix} 0 & v_n \\ v_n^* & 0 \end{pmatrix} = \begin{pmatrix} 0 & v \\ v^* & 0 \end{pmatrix}$$
$$T_n = T = \begin{pmatrix} 0 & 0 \\ 0 & w_n \end{pmatrix} = \begin{pmatrix} 0 & 0 \\ 0 & w \end{pmatrix}$$

Also, notice that:

$$U = Re(v)\sigma_x - Im(v)\sigma_y \text{ and } T = \tfrac{1}{2} w(\sigma_x - i\sigma_y)$$

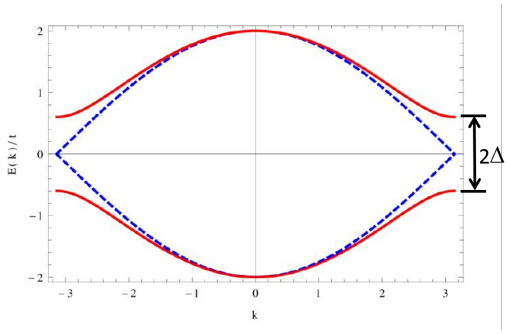


FIG. 2. Energy Spectrum of the Standard SSH Model. The red band is the energy spectrum for $v > w$, but the blue band is the energy spectrum when $v = w$, i.e., when the gap closes. This represents a topological phase transition occurring as mentioned in section III-B. Image taken from [6]


FIG. 3. Long Range SubLattice Hoppings in the Generalized SSH Model [7]

Finally, in momentum space:
$H(k) = h(k) \cdot \sigma = h(k)[\sigma_x + \sigma_y + \sigma_z]$
where $h(k) = \begin{pmatrix} 0 & d(k) \\ d^*(k) & 0 \end{pmatrix}$

Here, $d(k) = d_x + id_y$
$d_x = Re(v) + |w|cos(ka + arg(w))$
$d_y = -Im(v) + |w|sin(ka + arg(w))$

The energy spectrum $E(k)$ is $= \pm|d(k)|$, which is sketched out in figure 2 to the right [6].

### B. Setting up the Generalized SSH Model

Now, in analogy with the standard SSH Model, we say the generalized SSH Model [7] has momentum space representation such that:

$$H(k) = h(k) \cdot \sigma \text{ where } h(k) = \begin{pmatrix} 0 & d(k) \\ d^*(k) & 0 \end{pmatrix}$$

$d(k) = d_x + id_y = \sum_{-\infty}^{\infty} w_n e^{ink}$

Right now, the $w_n's$ seem a little mysterious. Let us convert to real-space using $|k> = \sum_{m=1}^{N} (e^{ikm}/\sqrt{N})|m>$

We introduce a change in notation here:

$$|n, A> = c_{n,1}^\dagger \text{ and } |n, B> = c_{n,2}^\dagger$$

$H$ becomes: $\sum_{m=1}^{N} \sum_{-n_l}^{n_r} (w_n^* |m+n, A>< m, B| + h.c)$

Now, we see that $w_n$ represents hopping amplitudes

from $A$ in the (m+n)-th cell to $B$ in the m-th cell.

One might have expected the sum for $n$ to run over $-\infty$ to $\infty$ in the Hamiltonian, but here we have to truncate amplitudes for the following reason: $h(k)$ will be treated as a continuous function even though $k(s)$ are quantized. This is a good approximation only when $|d'(k)/d(k)| << N/2\pi$, which can be shown to imply the sum for $d(k)$ can only run from $-n_l$ to $n_r$ [7].

Lastly, we briefly discuss sublattice (chiral) symmetry in the SSH Model. We have:

$\Gamma H = -H\Gamma$ where $\Gamma = \sum_{m=1}^{N} |m, A >< m, A| - |m, B >< m, B|$

In what follows, support is a mathematical term which, for our intents and purposes, means that the wavefunction would only be non-zero at certain sites (say the B sites). As an example, if an electron has a non-zero probability amplitude only on the B sites, it is is said to have support in B and no support in A. Now, the consequence of chiral symmetry is that if $|\psi >$ is an eigenstate of $H$ with energy $\epsilon$, then $\Gamma|\psi >$ is also an eigenstate with energy $-\epsilon$. So, for $\epsilon = 0$, we have degeneracy and we can construct $(1 \pm \Gamma)|\psi >$ states with support completely in sublattices A and B, respectively. Equivalently, if an eigenstate has support completely in A or B, then the energy must be zero since this implies $\Gamma|\psi >= \pm|\psi >$ [7]. These will be our robust zero-energy modes whose multiplicities we will count in section IV and find to be equal to the winding number calculated in III.

## III. WINDING NUMBER: THE TOPOLOGICAL INVARIANT OF INTEREST

We define the winding number $\nu$ and calculate it using Cauchy's residue theorem [6].
$\nu = (1/2\pi i) \int_{-\pi}^{\pi} \frac{d}{dk} ln(d(k)) dk$

and $ln(d(k)) = ln(|d|)e^{iarg(d)}$
Now, let $z = e^{ik}, dz = ie^{ik}dk, d(k) = f(z) = \sum_{-n_l}^{n_r} w_n z^n$.
This yields $\nu = (1/2\pi i) \oint_{|z|=1} f'(z)/f(z) dz$.

By fundamental theorem of algebra, we have: Here, $\epsilon_j$ is a root of this function and $\nu_j$ is the multiplicty of $\epsilon_j$
$z^{n_l} f(z) = \sum_{-n_l}^{n_r} w_n z^{n+n_l} = \Pi_j w_{n_r} (z - \epsilon_j)^{\nu_j}$

Substituting into the contour integral over the unit circle, we obtain $\nu = 1/(2\pi i) \oint_{|z|=1} (-n_l/z + \sum_j \nu_j/(z - \epsilon_j)$

Cauchy's residue theorem gives us $\nu = -n_l + \sum_{|\epsilon_j|<1} \nu_j$

Repeating the same process with $z = e^{-ik}$, we obtain
$\nu = n_r - \sum_{|\epsilon_j|<1} \nu_j$
where $\sum_{-n_r}^{n_l} w_{-n} z^{n+n_r} \propto \Pi_j (z - \epsilon_j)^{\nu_j}$

Equivalently, we can also use:
$\nu = -(1/2\pi i) \int_{-\pi}^{\pi} \frac{d}{dk} ln(d(k)^*) dk$

Using a similar procedure as before, we can show:
$\nu = -n_l + \sum_{|\epsilon_j|<1} \nu_j$ **(3.1)**

where $\sum_{-n_l}^{n_r} w_n^* z^{n+n_l} \propto \Pi_j (z - \epsilon_j)^{\nu_j}$

and $\nu = n_r - \sum_{|\epsilon_j|<1} \nu_j$ **(3.2)**

where $\sum_{-n_r}^{n_l} w_n^* z^{n+n_r} \propto \Pi_j (z - \epsilon_j)^{\nu_j}$

We will need equations 3.1 and 3.2 in section IV.

### A. Implicit Assumptions Made In Winding Number Calculation

One might ask why we did not consider possible roots lying on the unit circle, that is, with $|\epsilon_j| = 1$, while evaluating the contour integral. The reason is that if $z = e^{i\theta}$ for some $\theta$ is a root, it can be shown that $f(z) = 0$. We exclude the possibility that $d(k) = 0$ because we assume the energy spectrum to maintain a bulk gap. [7]

For simplicity, we must also assume the generalized SSH Model remains bipartite, that is, $A$ to $A$ and $B$ to $B$ hoppings are not allowed. If we allow for such hoppings, it can be shown the winding number calculated in this section is not invariant under adiabatic transformations. [7] The diagonal entries in the 2 x 2 Hamiltonian in momentum-space representation will not be zero as before. In such an event, $h(k)$ can be continuously deformed into new configurations with different winding numbers. Thus, it would not serve as a "good" number to classify topologically equivalent Hamiltonians. We would have to find a new topological invariant that describes such systems (that do not have chiral symmetry). Finding appropriate topological invariants for different systems is one of the biggest challenges of the subfield of condensed matter physics that attempts to understand topological matter. For further reading, the interested reader may refer to the Periodic Table of Topological Invariants. [8]

### B. Aside: Topological Phase Transition in the Standard SSH Model

Since we have developed the machinery to calculate the winding number, we can now present a result mentioned in section I. In the standard SSH Model, we can show $\nu = 1$ if $|w| > |v|$ and $\nu = 0$ if $|w| < |v|$. [6] Thus, trusting the bulk-edge correspondence, we expect the two different Hamiltonians to be topologically and physically inequivalent, since they have different winding numbers. Indeed, it can be shown that the standard SSH Model with $|w| < |v|$ cannot be smoothly deformed into one with $|w| > |v|$. The physical consequence of this mathematical

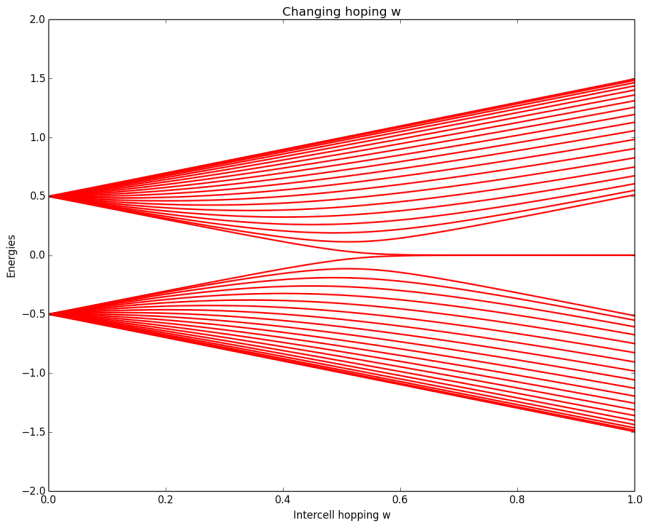


FIG. 4. We fix $v$ to be 0.5 (Intra-Cell Hopping) and vary $w$ (Inter-Cell Hopping) from 0 to 1. We observe the system transitions from being an insulator to a metal as $w \approx v$ and goes back to being an insulator as the gap re-opens. This is an example of a topological phase transition [6].

inequivalence is that the gap between the energy bands closes and re-opens. The system is said to undergo a topological phase transition at $|w| = |v|$. See Figure 4.

## IV. CALCULATING ROBUST ZERO ENERGY EDGE MODES

Since our goal is to study how many eigenstates can be localized at the edges, we purposely do not use periodic boundary conditions. This makes the finiteness of the chain manifest. In one of our homework sets, we see how open boundary conditions give us the same energy spectrum and the same observables in the $N$ goes to $\infty$ limit. Here, since we want to understand the behavior at the edges of a finite chain, we do not want to make them equivalent by applying PBC. For all we know, some interesting finite N behavior might get lost in the process. In the large N limit, the boundary conditions do not make a difference and that is why we use PBC –for ease of calculation. In our case, we treat our system as it is, which is a finite, open chain. Now, let there be N unit cells.

$$H = \sum_{m=1}^{N}(w_0^*|m, A><m, B| + h.c)$$
$$+\sum_{n=1}^{n_r}\sum_{m=1}^{N-n}(w_n^*|m+n, A><m, B| + h.c)$$
$$+\sum_{n=1}^{n_l}\sum_{m=n+1}^{N}(w_{-n}^*|m-n, A><m, B| + h.c)$$

We want to solve the eigenvalue problem:

$$H|\psi>=\epsilon|\psi>$$

As usual, let $|\psi>=\sum_{m=1}^{N}(a_m|m, A> + b_m|m, B>)$

We plug in our ansatz into the Hamiltonian to find 2N sets of linear equations for 2N variables $a_m, b_m, m = 1, .., N$
Sparing some gory details of algebra, we discuss the results.
For $a_m$, we have:
$\sum_{n=1-m(>-n_l)}^{n_r} w_n a_{m+n} = \epsilon b_m$ for $m = 1, .., n_l$ **(4.1)**
$\sum_{n=-n_l}^{n_r} w_n a_{m+n} = \epsilon b_m$ for $m = n_l + 1, .., N - n_r$**(4.2)**
$\sum_{n=-n_l}^{N-m(<n_r)} w_n a_{m+n} = \epsilon b_m$ for $m = N - n_r + 1, .., N$ **(4.3)**

We are looking for zero energy modes $\epsilon = 0$, which allows us to decouple $a_m$ and $b_m$, which is a consequence of chiral symmetry discussed in section II.

Solving for $a_m$, plug in the ansatz $a_{m+n} = \eta^n$ like we have in class/homeworks before. From 4.2, we have $\sum_{n=-n_l}^{n_r} w_n \eta^n = 0$

This equation is familiar to us from section III. Roots of this equation are the same $\epsilon_j$ in equation 3.1. Thus, $a_m = \epsilon_j^m$. It can be shown that any linear superposition of $m^l \epsilon_j^m, l = 0, 1, .., \nu_j - 1$ is also a solution of the equation above [7]. We omit the proof here. Now, we try to plug this ansatz into 4.1 and 4.3. This set of equations can be solved numerically. We discover that they do not always have solutions for $\epsilon = 0$. So, zero energy modes do not necessarily exist in finite systems. But when $N \to \infty$, these three sets of equations show that there are a total of $-n_l + \sum_{|\epsilon_j|<1} \nu_j$ non-zero solutions localized at the left edges, exponentially decaying as we move towards the right, provided $\nu > 0$. From our discussion in section II, we can construct states localized completely in sublattice A at the left edge and decaying as we move to the right, owing to chiral symmetry. We just need to set $b_m$=0.
And when $\nu \leq 0$, we find that we get no left-edge modes. Equation 4.1 gives more constraints than there are candidate solutions that can decay towards the right edge. So, we look for localized right-edge modes that exponentially decay towards the left edge. The equations we use are in analogy with 4.1 -4.3. For $b_m$, we have:

$\sum_{n=-n_l)}^{m-1(<n_r)} w_n^* b_{m-n} = \epsilon a_m$ for $m = 1, .., n_r$
$\sum_{n=-n_l}^{n_r} w_n^* b_{m-n} = \epsilon a_m$ for $m = n_r + 1, .., N - n_l$
$\sum_{n=m-N(>-n_l)}^{n_r)} w_n^* b_{m-n} = \epsilon a_m$

for $m = N - n_l + 1, .., N$

Then, proceeding as before and taking the $N \to \infty$ limit, we get $n_r - \sum_{|\epsilon_j|<1} \nu_j$ localized right edge zero energy modes with support purely in sublattice $B$, which we know is equal to the winding number according to equation 3.2.

Thus, for the generalized 1D SSH Model, we see that localized non-zero energy modes might not necessarily exist for finite $N$. However, they do exist in the thermodynamic limit and are equal to the winding

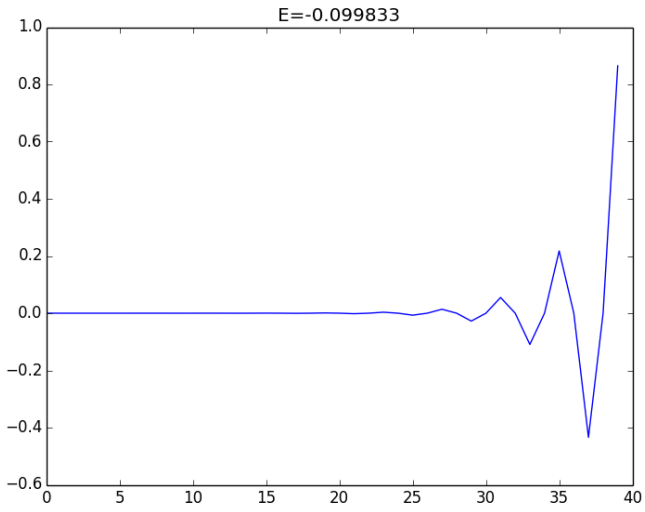


FIG. 5. Edge Modes In a Finite Chain: x-axis represents no. of sites in our 1D chain and y-axis represents amplitude of a localized right edge mode for $\epsilon \approx 0$.[6]

number. [7] This proves the bulk-edge correspondence in the thermodynamic limit for the generalized SSH Model.

## V. ADDITIONAL CONSIDERATIONS FOR A MORE COMPLETE PROOF

In our discussion, we did not consider the existence of edge modes with non-zero energy. We know they do not contribute to the winding number since we saw the winding number is equal to the number of zero-energy modes in the thermodynamic limit. But the bulk-edge correspondence would be weakened, in some sense, if there were robust non-zero energy modes that the winding number did not account for. It turns out that non-zero energy modes are, in fact, not robust to smooth deformations of the Hamiltonians. Using first order perturbation theory, it can be shown that these modes undergo an energy shift and de-localize over the lattice. [7]

Secondly, we implicitly considered deformations of the Hamiltoninan by changing $h(k)$, which effectively meant smoothly deforming $d(k)$. But we can also consider spatial deformations such that $w_n$ becomes $w_n + \delta w_n$. It can be shown that zero energy eigenmodes remain eigenmodes of the deformed Hamiltonian up to first order in perturbation theory as long as deformations are appropriately small enough. [7]

Thirdly, we tacitly assumed $d(k) \neq 0$ so that the bulk energy gap remains open as we deform our Hamiltonian. The integral for the winding number needs to be evaluated with care in the case of level crossing, which is a complication we circumvented. [1]

Lastly, from the perspective of pedagogy and presentation, one might ask why we could not have simply used PBCs since we were going to prove the bulk-edge correspondence in the thermodynamic limit anyway. We choose to use open-boundary conditions to explicitly show how one could go about finding the eigenstates in this case, but more importantly, to show that zero energy states do not always exist for physical, finite, open chains.

For further reading on the same, please refer to [1], [6] and [7].

## VI. CONCLUSION

In this article, we discussed one formulation of the bulk-edge correspondence in terms of relating robust edge modes with topological invariants. We saw that the number of zero-energy modes in the generalized SSH Model is equal to the winding number, in the thermodynamic limit. We also discussed a powerful physical consequence of classifying Hamiltonians as topologically equivalent and finding topological invariants associated with them – the standard SSH Model undergoes a phase transition as the intracell hopping becomes greater than the intercell hopping (or vice versa) and this is characterized by the winding number of the two model Hamiltonians being different. Lastly, we discussed important technical aspects of our developments, the assumptions made in the proof outlined, and what would need to be taken into account for a more complete proof.

## VII. REFERENCES

**[1]** D. Tong, Lecture Notes, Quantum Hall Effect, January 2016
**[2]** W. Rudin, Principles of Mathematical Analysis, (McGraw-Hill, New York 1976)
**[3]** J. Sau, Bulk-Edge Correspondence in the Kitaev Chain, 2021
**[4]** S. Ryu, 10 Symmetry Classes and the Periodic Table of Topological Insulators, 2021
**[5]** W. P. Su, J. R. Schrieffer, A. J. Heeger, "Solitons in Polyacetylene," Phys. Rev. Lett. 42, 1698 (1979)
**[6]** B.C Zhu, J. Asboth, L. Oroszlany, A. Palyi, Lecture Notes, Topological Insulators, Spring 2013
**[7]** B. H. Chen, D. W. Chou, "An Elementary Rigorous Proof of Bulk-Boundary Correspondence in the Generalized SSH Model," Phys. Lett A 384, 126168 (2020)
**[8]** S. Ryu, A. P. Schnyder, A. Furusaki and A. W. W. Ludwig, "Topological insulators and superconductors: Tenfold way and dimensional hierarchy," New J. Phys. 12, 065010 (2010)
Web-addresses for references **[1], [3], [4]** in order:
https://www.damtp.cam.ac.uk/user/tong/qhe/qhe.pdf
https://topocondmat.org/ [If link does not work, please

search for the site address and look for Bulk-Edge Correspondence in Kitaev Chain page]
https://topocondmat.org/ [If link does not work, please search for the site address and look for 10 Symmetry Classes and Periodic Table of Topological Insulators page]